crystals

MDPI

Article

How Microanalysis Can Be Discriminant on Black Pompeian Wares

Laura Medeghini [1,*], Silvano Mignardi [1], Giorgia Di Fusco [1], Michela Botticelli [1], Fulvio Coletti [2] and Caterina De Vito [1]

[1] Department of Earth Sciences, Sapienza University of Rome, P.le A. Moro 5, 00185 Rome, Italy; silvano.mignardi@uniroma1.it (S.M.); giorgia90df@gmail.com (G.D.F.); michela.botticelli@uniroma1.it (M.B.); caterina.devito@uniroma1.it (C.D.V.)

[2] Archaeological Park of the Colosseum, Piazza di S. Maria Nova 53, 00185 Rome, Italy; fulvio.coletti@uniroma1.it

* Correspondence: laura.medeghini@uniroma1.it

Received: 31 August 2020; Accepted: 26 September 2020; Published: 28 September 2020

Abstract: In the present work the advantages of punctual approaches are discussed in the discrimination of black wares from the Sanctuary of Venus Fisica (Pompeii, Italy), dated between the 2nd and 1st century BC. Black-gloss ware and "bucchero" samples are analyzed by a multi-analytical approach including optical microscopy (OM), X-ray powder diffraction (XRPD), scanning electron microscopy with Energy Dispersive Spectroscopy (SEM-EDS) and electron microprobe analysis (EMPA) to investigate the mineralogical and petrographic features of these artefacts. Grain size, firing conditions and potter's expertise influenced the final appearance of the superficial decorative black layer. In addition, punctual chemical analysis was fundamental to verify the archaeological indication of specific production sites.

Keywords: Pompeii; archaeometry; black-gloss ceramics; bucchero; microanalysis; point analysis

1. Introduction

In Greek and Roman Antiquity metallic objects were considered renown goods, symbol of wealth. This is true not only for rich metals but also for iron and bronze artefacts used for weapons, vessels and ornamentation which had a symbolic meaning. Dishes, vessels, and flatwares, mainly made of bronze during the Etruscan Age and silver in the Roman Age, were put in tombs as grave goods. In ancient times, as at present, people who could not afford such production loved having goods that could give the illusion of wealth, of belonging to the upper class. In this background, connected to the need of gratifying the aspirations of a large slice of buyers, the production of black-gloss ware and "bucchero" is included, their aesthetic value being due to the shiny black color of their surfaces [1,2]. In fact, "bucchero", produced in Etruria, Latium, and Campania since the mid-7th century BC, and later attic black-gloss ware, since the end of the fifth century BC, originally imposed themselves on the Mediterranean markets in replacement of metal artefacts, following the crisis in the metal manufacturing especially of the Elba island, on the coast of Vetulonia and Corsica [3,4].

Black-gloss ware (BGW) was an ancient fine ceramic used as table ware, firstly produced in Greece from the fifth century BC (attic black-gloss ware) [5]. It spread in all the Mediterranean world from the 4th to the 1st century BC [6]. "Campanian pottery" is the typical Italian production imitating attic black-gloss ware. Basing on morphological features, it was distinguished into "Campanian A" with a red ceramic body, "Campanian B" with a light brown or yellowish ceramic body, and "Campanian C" with a grey matrix [7]. In addition, numerous local imitations were included in other groups labelled as "B-oid" and "g/g wares" (grey wares) [8]. Compactness, color shadows and slip are used to distinguish

different specialized production areas, including Campania, Cales, Etruria, Pyrgi, Apulia, Latium, and Pompeii [9,10].

Either scientific analysis or experimental approaches [11–13] on black-gloss ware [14–17] suggested that the slip was produced by a fine suspension of refined clay applied to the dry surface and then fired following an oxidizing–reducing–oxidizing cycle forming nanoparticles of magnetite (Fe_3O_4), wustite (FeO) or hercynite ($FeAl_2O_3$) [18].

Bucchero, instead, belongs to the Etruscan production developed between the 7th and 5th century BC, exported to Campania and most of the Mediterranean area. The most ancient type is "Bucchero sottile" from the production centers of the southern Etruria followed by "Bucchero pesante", mainly produced in the northern sites. Bucchero is characterized by an intense black color, both on the surface and in fracture [19]. Its presence in Pompeii is attested around the end of the 6th century BC, especially in the sacred areas of the Forum such as the Temple of Apollo [20,21].

Different possible procedures were proposed to explain the uniform black nature of this pottery, such as the mixing of charcoal powder or MnO_2 with the clay, a process of fumigation, or the sole firing in a reducing atmosphere [22].

Even if the reason of their use and production could be similar, aesthetic features, color, and shine are different due to the raw materials and technological processes they underwent, that can be reconstructed thanks to archaeometric investigations [23,24]. Mineralogical, petrographic, and chemical methods are usually applied on ancient ceramic material with this purpose [25–28], combining bulk (e.g., X-ray powder diffraction (XRPD) [29], thermo gravimetric analysis (TGA) [30], Fourier transform infrared spectroscopy (FTIR) [31], X-ray fluorescence (XRF) [32], instrumental neutron activation analysis (INAA) [33,34], etc.) and punctual techniques (scanning electron microscopy (SEM-EDS) [35], electron microprobe analysis (EMPA) [36], Raman spectroscopy [37,38], secondary ion mass spectrometry (SIMS) [39], etc.). Being a ceramic material, heterogeneous, bulk analyses have been preferably applied in the archaeometric approach, as this is considered more representative of the whole composition of the artefact. However, recent works have highlighted the important support and advantages of punctual analysis, particularly concerning provenance studies [40–42], technological studies [43], and analysis of slip and superficial decorations [44,45].

The main aim of this work is to provide new scientific data concerning the mineralogical, petrographic, and chemical composition of black ceramics found in Pompeii, highlighting the contribution of micro-analysis in reaching this important task. Particularly, they can provide information on mineral markers useful to trace the provenance as well as to give an overall picture of the *chaîne opératoire* related to the superficial decorative black layer.

2. Geological and Archaeological Context

The ancient city of Pompeii occupies the southern part of the Campanian Plain, at an altitude of about 30 m amsl, between Somma-Vesuvius to the north, the mouth of the Sarno river to the south and the coastline to the west. This particular position, at the central-southern sector of the Gulf of Naples, was favourable to commercial exchanges with the western and eastern Mediterranean and to the creation of a port. Recent researches have ascertained that this port was located in the lagoon created by the undertow of the estuary of the Sarno river, south of Regio VIII, in the lowest levels of the alluvial valley between the substructures of the temple of Venus Fisica and Piazza Esedra of the modern site of Pompeii [46,47].

The Plain is a part of depression (graben) emerged from the Pliocene (some 5 Ma ago) and after the lowering of limestone blocks, whose remains still emerge (south of the Sorrento Peninsula), it was partly filled with sedimentary and volcanic products [48].

Reddish and blackish blistering lava and scoriae with phenocrysts of leucite and augite (Vulcaniti della Civita), emitted by the nearby Vesuvius, outcrop in the archaeological site [49].

The Sanctuary of Venus Fisica occupies Insula I inside Regio VIII, close to one of the most important areas of Pompeii, characterized by the presence of public and political buildings such as the Basilica,

the Forum, and the Porta Marina (Figure 1). The original building, an ionic tetrastyle temple, was built in the second half of the 2nd century BC. In the second phase, during the tyrannical period of Lucius Cornelius Sulla (88–80 BC), the sanctuary had small changes and restorations in the architectural order, while a phase of major renovations took place in the Julian Claudian Age. The earthquake of 62 AD deeply damaged it. Therefore, at the time of the eruption on August 24th of 79 AD the sanctuary was a construction site where reconstructions were being carried out [50,51].

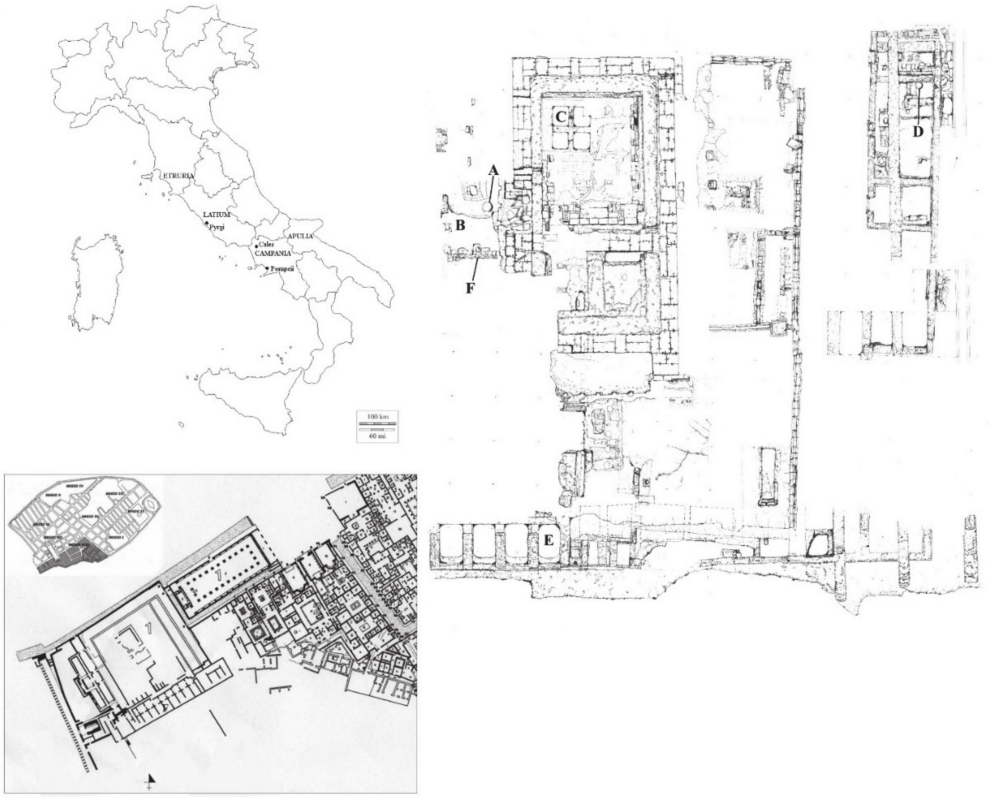

Figure 1. Map of main production sites (**top left**), localization of the Temple of *Venus Fisica* (**bottom left**) and map of the archaeological site (**top right**). B is identified as the place where the analyzed samples of black-gloss ware and bucchero come from.

Archaeological investigations identified different types of votive contexts where black-gloss ceramics always appear among the main objects of the rite. Votive potholes, pits with discharge of sacra from the temple, rooms in foundations with votive elements to celebrate the re-consecration of the sanctuary, votive basins and remains of destructed underground spaces with votive drains were identified. They have revealed a large number of "sacra" and "ex votos" that, periodically, had to be disposed of in pits placed outside the temple, but within the walls of the "themenos" (everything that was present in the consecrated area, could not be taken elsewhere), to give space to other gifts that accumulated over time [52].

3. Materials and Methods

The pottery of the temple of Venus in Pompeii refers to two successive contexts. Discovered within open pits filled with the discharge of materials, the vases were originally "ex votos" displayed in the temple and dedicated to the divinity, dated during the first phase of the temple (140–130 BC) and used also under Sulla. In addition to the dating material, the excavations of both contexts have discovered even older vases, such as bucchero vases dating back to the 5th century BC or Apulian black-gloss ware dating to the 4th (Table 1).

Table 1. Macroscopic classification and hypothesized provenance considering typology and macroscopic features of each sample under investigation.

Samples.	Shape	Production	Macroscopic Analysis of Gloss
4026-102	*Kylix*	Central Italy	Very thin layer of black paint with iridescent reflections and shades of green
4032-101	plate	Southern Etruria, Pyrgi	Very thin layer of black paint that, in direct light, shows a strong iridescence with green tones
4032-158	plate	Southern Latium	Very thin layer of black paint, with a slight blue-green iridescence
4226-106	plate	Cales	Black gloss with reflections in shades of green
4032-103	*Kylix*	Apulia	Altered black gloss
4032-105	*Skyphos*	Pompeii	Cup with black paint with a weak iridescence of the blue-green paint. The foot shows traces of a reddish coating
4032-104	plate	Pompeii	Very fine black paint, well preserved, with iridescent reflections tending to blue
4226-108	Stemmed bowl	Pompeii	Bucchero
4226-109	*Rasmussen* 1979—3a	Pompeii	Bucchero
4226-110	cup	Pompeii	Bucchero
4020-107	*Rasmussen* 1979—2	Pompeii	Bucchero

Eleven ceramic samples were selected by the archaeologists considering functional classifications, contextual stratigraphic origin and macroscopic features to be representative of the materials found and then analyzed by a multi-analytical approach including optical microscopy in thin section (OM), X-ray powder diffraction (XRPD), scanning electron microscopy with Energy Dispersive Spectroscopy (SEM-EDS) and electron microprobe analysis (EMPA).

Petrographic analysis was performed using a D-7082 Oberkochen microscope (Carl Zeiss, Oberkochen, Germany) to define main inclusions, voids and matrix features according to the Whitbread's procedure [53].

On the basis of petro-fabrics identified by OM, a micro-sample of eight representative samples from the ceramic body was gently ground in an agate mortar and analyzed by XRPD using a D8 FOCUS diffractometer (Bruker, Karlsruhe, Germany) with CuKα radiation, operating at 40 kV and 30 mA. The following instrumental set-up was chosen: 3–60° 2θ range, scan step of 0.02° 2θ/2s. Semi-quantitative analysis was performed using XPowder X© Ver. 2019.06.22 software, based on the "Reference Intensity Ration Method".

Thin sections were metallized to be analyzed by a Quanta 400 (SEM-EDS) instrument (FEI company, Hillsboro (OR), USA), operating at 20 kV, equipped with an EDAX Genesis detector for chemical analysis. EDS spectra were acquired to analyze the chemical composition of both the black surface and the inclusions. A minimum of three spectra were collected for each matrix and slip. In addition, SEM imaging was performed to study the ceramic micro-morphology and the vitrification degree of the black superficial layer [35].

A SX50 electron microprobe (Cameca, Gennevilliers, France) equipped with five wavelength-dispersive spectrometers was also used to analyze in detail the chemical differences among ceramic body and black-gloss in black-gloss ware samples (7, Table 1). A minimum of three spots on both body and slip were collected and then the average concentration was calculated for each

element. The following operating conditions were chosen: accelerating voltage 15 kV, beam current 15 nA, and beam size 10 µm on the matrix and 5 µm on the glaze. Element peaks and background were measured with counting times of 20 and 10 s respectively. Wollastonite was used as a reference standard for Si (TAP, thallium (acid) phthalate crystal) and Ca (PET, pentaerythriol crystal), periclase for Mg (TAP), corundum for Al (TAP), jadeite for Na (TAP), rutile for Ti (PET), magnetite for Fe (LIF, lithium fluoride crystal), rhodonite for Mn (LIF), orthoclase for K (PET), chalcopyrite for Cu (LIF), galena for Pb (PET), cassiterite for Sn (PET), and sphalerite for Zn (LIF).

Matrix corrections were calculated by the PAP method [54], with software supplied by Microbeams Services (Gennevilliers, France). The analytical error was ~1% relative for major elements, and it increased as their concentration decreases. Detection limits under the specified working condition ranged between 0.01 and 0.1 wt.%.

4. Results

4.1. Ceramic Body

4.1.1. OM Analysis

Petrographic analysis allowed the identification of 2 fabrics showing similar features in terms of inclusions, voids and matrix (Table 2 and Figure 2): "fabric A-fine" from silt to sand and "fabric B-coarse" from silt to coarse sand.

Table 2. Microscopic features and petrographic composition of the ceramic samples analyzed.

Samples	Porosity	Matrix	Inclusions
FABRIC A 4026-102	10% micro-vesicles micro-/meso-vughs	70% optically inactive	20% Dominant: quartz (0.02–0.2 mm), plagioclase (0.02–0.1 mm) Common: mica (0.02–0.2 mm), nodules of iron oxides (0.02–0.15 mm) Rare: calcareous inclusions (0.02–0.8 mm)
4226-106	5% micro-vesicles micro-/meso-vughs	80% optically inactive	15% Dominant: quartz (0.01–0.15 mm), plagioclase (0.01–0.1 mm) Rare: nodules of iron oxides (0.02–0.15 mm) Very rare: destabilized calcite (1 mm)
4032-101	10% micro-/meso-vesicles meso-/macro-vughs	70% optically inactive	20% Dominant: quartz (0.02–0.2 mm), plagioclase (0.02–0.1 mm) Common: mica (0.02–0.2 mm), nodules of iron oxides (0.02–0.15 mm) Rare: calcareous inclusions (0.02–0.8 mm)

Table 2. *Cont.*

Samples	Porosity	Matrix	Inclusions
4032-158	20% micro-/meso-vesicles micro-/macro-vughs	60% optically inactive	20% Dominant: quartz (0.1–0.15 mm), plagioclase (0.15–0.01 mm) Common: mica (0.01–0.08 mm), nodules of iron oxides (0.01–0.04 mm)
4032-105	10% micro-/meso-vesicles micro-/macro-vughs	70% optically inactive	20% Dominant: quartz (0.02–0.1 mm), plagioclase (0.02–0.05 mm) Common: pyroxene (0.5–0.12 mm), mica (0.02–0.1 mm) Rare: nodules of iron oxides (0.02–0.2 mm)
4032-104	10% micro-vesicles micro-/macro-vughs	70% optically inactive	20% Dominant: quartz (0.02–0.2 mm), plagioclase (0.05–0.15 mm) Common: mica (0.02–0.5 mm) Rare: fragments of rocks (0.01 mm)
4226-108	10% micro-/meso-vesicles micro-/macro-vughs	60% optically inactive	20% Dominant: quartz (0.01–0.25 mm), plagioclase (0.05–0.1 mm) Common: mica (0.03–0.1 mm)
4020-107	10% micro-vesicles micro-/mega-vughs	60% optically active	30% Dominant: quartz (0.01–0.08 mm), plagioclase (0.05–0.2 mm) Common: mica (0.01–0.2 mm), Rare: nodules of iron oxides (0.02–0.1 mm)
FABRIC B 4226-109	20% micro-/meso-vesicles micro-/meso-vughs	50% optically active	30% Dominant: quartz (0.02–0.15 mm) Common: plagioclase (0.05–0.1 mm), K-feldspar (0.02–0.4 mm), mica (0.01–0.2 mm) Rare: fragments of calcareous rocks (0.07–0.2 mm)

Table 2. *Cont.*

Samples	Porosity	Matrix	Inclusions
4226-110	30% micro-/macro-vesicles micro-/meso-vughs	30% optically active	40% Dominant: quartz (0.01–0.2 mm), plagioclase (0.05–0.2 mm) Common: mica (0.03–0.1 mm) Rare: fragments of rocks (0.1–0.2 mm), fragments of calcareous rocks (0.07–0.2 mm)
loner 4032-103	20% micro-/meso-vesicles micro-/macro-vughs	60% optically inactive	20% Dominant: quartz (0.02–0.1 mm), plagioclase (0.05–0.2 mm) Microfossils Common: pyroxene (0.15–0.6 mm), fragments of basic rocks (0.05–0.4 mm) Rare: fragments of basic rocks (0.1–0.6 mm), fragments of calcareous rocks (0.02–0.15 mm)

The fabric A-fine (samples 4026-102, 4226-106, 4032-101, 4032-158, 4032-105, 4032-104, 4226-108, and 4020-107) showed a predominance of quartz and plagioclase, with mica and pyroxene (present), rare nodules of iron oxides, and lithic fragments such as flint and calcareous rocks. The porosity is mainly represented by micro- and meso-vesicles and from micro- to macro-"vughs" aligned to the margin of the section.

Samples 4226-109 and 4226-110 are included in the fabric B-coarse characterized by "coarser" inclusions respect to fabric A-fine. Quartz is the main inclusion, along with plagioclase, K-feldspar, mica, and rare fragments of calcareous rocks. Porosity includes micro- and macro-vesicles and from micro- to meso-vughs oriented in parallel along to parallel to the margin of the sample.

Finally, sample 4032-103 is a loner and is distinguished from the other samples for some fragments of basic rocks with grain size in the range 0.05–0.4 mm and microfossils (planktonic foraminifera) both scattered in the matrix and embedded in carbonate clasts.

4.1.2. XRPD Analysis

The samples are characterized by very abundant quartz (Table 3). In addition, XRPD spectra of samples belonging to fabric A-fine showed the common presence of pyroxene, traces of mica and variable amounts of K-feldspars and calcite. The bucchero sample in this fabric is characterized by high amounts of mica and K-feldspar, whereas pyroxene is absent.

The samples of bucchero belonging to fabric B-coarse displayed a minor amount of plagioclase, K-feldspar, and mica. Traces of calcite are also present.

The XRPD spectrum of the loner sample 4032-103 confirmed the presence of plagioclase, pyroxene, and calcite in scarce amount and mica in traces.

Finally, clay minerals were not identified, neither in traces, in any sample, whereas neo-formed gehlenite was identified, as present or in trace, only in black-gloss ware samples.

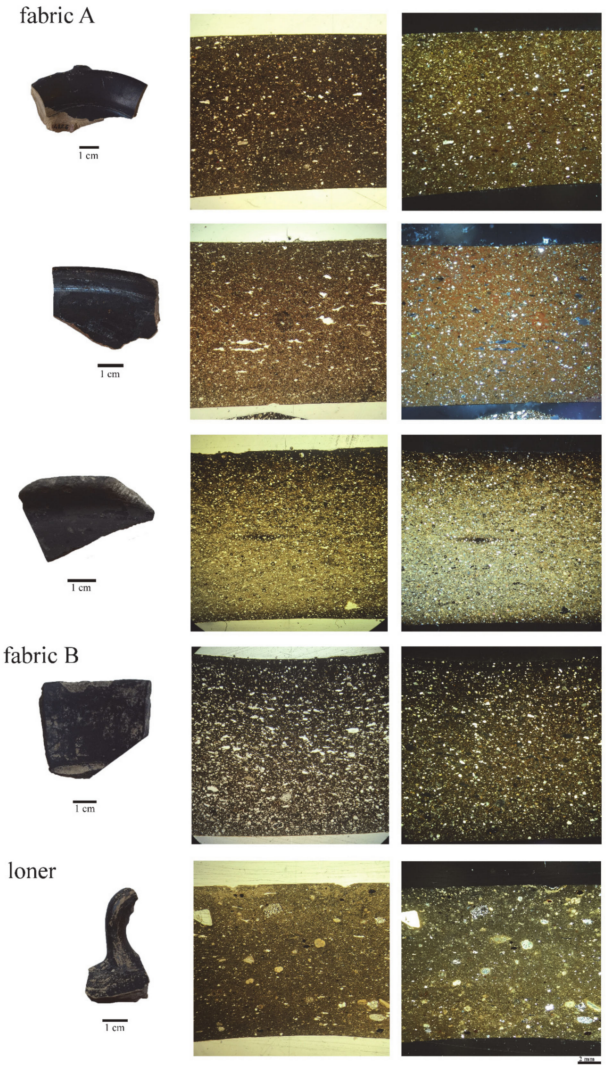

Figure 2. Microscopic images of representative samples for each fabric, from top to bottom: sample 4026-102 (fabric A-fine, Black-Gloss Ware), sample 4032-104 (fabric A-fine, Black-Gloss Ware), sample 4020-107 (fabric A-fine, Bucchero), sample 4026-110 (fabric B-coarse, Bucchero), sample 4032-103 (loner, Black-Gloss Ware).

Table 3. Mineralogical composition of bucchero and black-gloss ware (BGW) samples.

Sample		Fabric	Qtz	Pl	Px	Cal	Mca	Hem	Kfs	Gh
4026-102	BGW	A	++++	+++	+	+	tr	+	+	tr
4032-158	BGW		++++	++	++		tr	+		tr
4032-105	BGW		++++	+++	++	++	tr	tr		+
4032-104	BGW		+++	+++	++		tr	+	++	
4226-108	Bucchero		++++	+++			+++		+++	
4226-109	Bucchero	B	++++	++		++	+		+	
4226-110	Bucchero		++++	+		tr	++		+	
4032-103	BGW		++++	+++	++	++	+			+

Semiquantitative indications are: ++++ very abundant (70–50%), +++ abundant (50–30%), ++ present (30–15%), + scarce (15–5%), tr trace (<5%). (Qtz: quartz; Pl: plagioclase; Px: pyroxene; Cal: calcite; Mca: mica; Hem: hematite; Kfs: K-feldspar; Gh: gehlenite).

4.1.3. SEM-EDS Analysis

SEM images and EDS spectra confirmed the results of the previous analysis and provided deeper information about the fine inclusions embedded in the matrix, as well as preliminary chemical data of the body. Indeed, samples of black-gloss ware included in fabric A-fine revealed the predominance of mineral inclusions such as quartz, K-feldspar, clinopyroxene, biotite, Ca-plagioclase (sample 4032-101) amphibole (sample 4026-102), and zircon (samples 4032-158 and 4032-101).

The matrix of the ceramic body showed high amounts of Si and Al and minor amounts of Fe, K, Ca, and Mg for those samples identified as produced from central Italy, Pyrgi, and Southern Latium; the sample identified as produced at Cales showed high amounts of Ca in the ceramic body, whereas samples from Pompeii have low amounts of Ca.

In addition, the elemental distribution in the X-ray maps of sample 4226-106 (Figure 3) shows a 2–5 μm thick rim at the calcareous inclusion/matrix interface composed of Al together with Ca and Si, gehlenite formed only at the edge of a calcareous inclusion which preserves an unaltered nucleus.

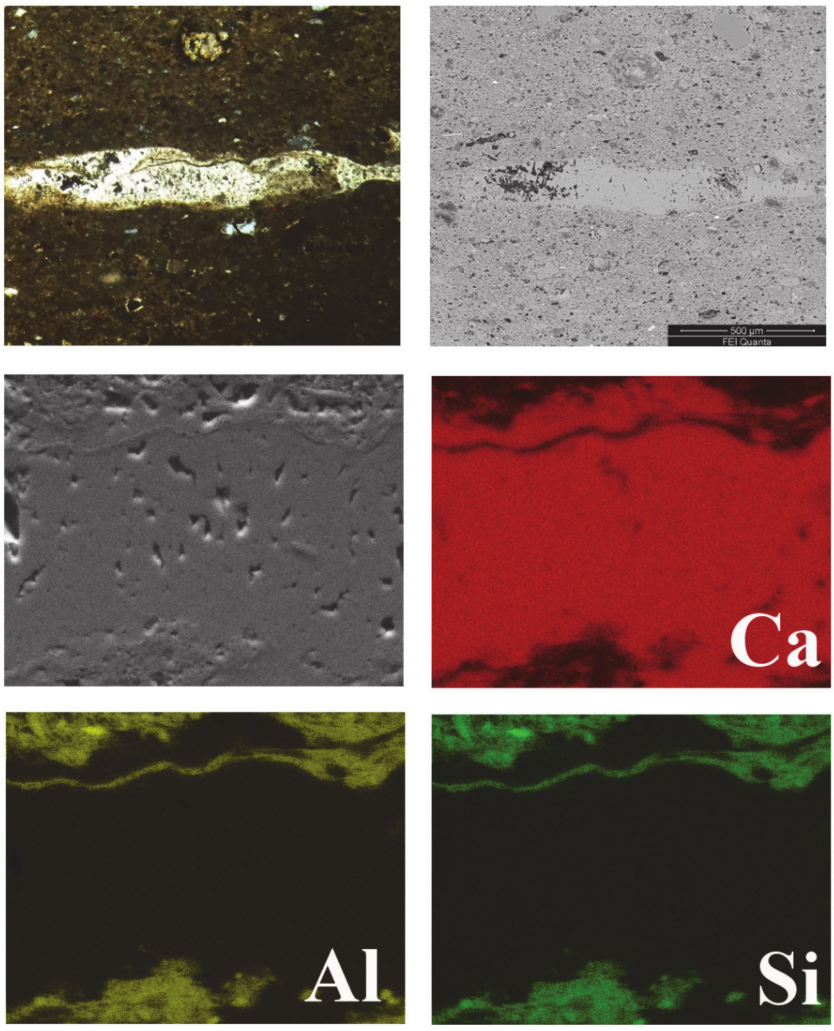

Figure 3. Optical microscopy (OM) and Back Scattered Electron (BSE) images of destabilized calcareous inclusion. Secondary Electron (SE) image and X-ray maps of the reaction rim (sample 4226-106).

The bucchero samples belonging to fabric A-fine showed a matrix of the ceramic body with high Si, Al, lower amount of Fe and traces of Ca, K, and Mg. Inclusions are mainly composed of quartz, K-feldspar, plagioclase, mica, and very small inclusions of zircon and garnet. In addition, sample 4020-107 showed planktonic or benthic foraminifera scattered in the ceramic body.

SEM-EDS analysis on the bucchero samples belonging to fabric B-coarse (4226-109 and 4226-110) revealed the presence of quartz, K-feldspar, zircon, and garnet as inclusions. The matrix showed a chemical composition with high Si, Al, and low amount of Fe, Ca, and K.

Concerning the "loner" (sample 4032-103), the presence of clinopyroxene, nodules of iron oxides, ilmenite, fragments of flint, and planktonic or benthic foraminifera (among them, *Globigerinoides* were identified, Figure 4), confirm the different composition of this sample with respect to the other samples. The matrix of the ceramic body is mainly composed of Si, Al, and Ca, with low amounts of Fe and traces of K and Mg.

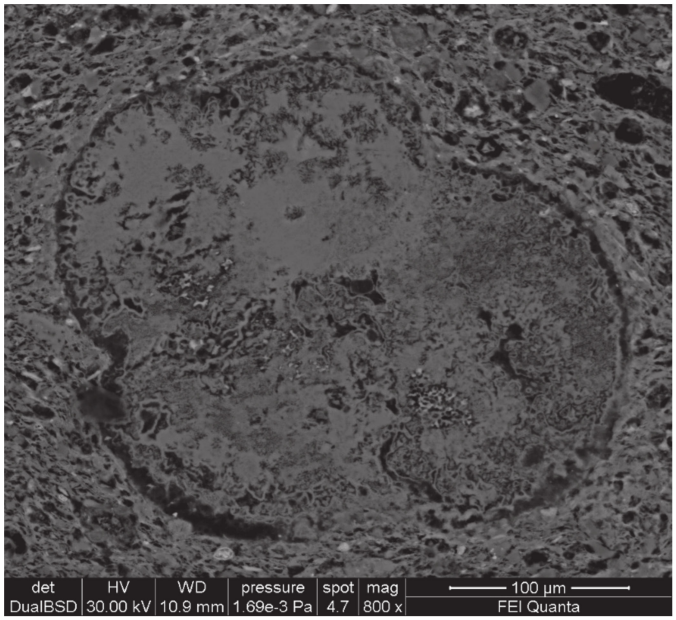

Figure 4. BSE image of a *Globigerinoides* microfossil identified in sample 4032-103 (loner, Black-Gloss Ware).

4.2. Slip

4.2.1. OM Analysis

Based on the different features of the superficial layer it was possible to separate samples in two groups. The samples belonging to the first group, identified as black-gloss ware (4026-102, 4226-106, 4032-101, 4032-158, 4032-105, 4032-104, and 4032-103), showed a very thin layer (about 0.01 mm thick) with good adhesion to the substrate. The color in plane polarized light (PPL) was dark brown/black or grey and from yellow-greenish to black in crossed polarized light (XPL). Sometimes, the color in XPL changed rotating the stage. On the contrary, the samples identified as bucchero (4226-108, 4020-107, 4226-109, and 4226-110) are characterized by the absence of a superficial coating or by a thin layer (about 0.1 mm thick), black in PPL and dark reddish-brown in XPL.

4.2.2. SEM-EDS and EMP Analyses

Chemical composition of the slip was obtained by the combined results of SEM-EDS and EMPA. In addition, SEM investigations highlighted different levels of vitrification of the slip among the samples.

The slip is composed of a single layer, being it very compact in the case of black-gloss ware (Figure 5a,b) and more porous, inclusion-bearing in the bucchero samples (Figure 5c). Samples of black-gloss ware of fabric A-fine showed a compact superficial layer, with a variable thickness from 9 to 15 µm, and chemical composition similar to the matrix, but with lower amounts of Si and Ca and higher of Al and Fe. The bucchero samples belonging to fabric A-fine showed an irregular surface layer, with a thickness of about 160 µm, not vitrified, but characterized by the presence of a series of embedded

inclusions. Among them, K-feldspars (particularly, a high T feldspar with a disordered structure embedding Fe inclusions), clinopyroxene, and apatite were identified. Fabric B-coarse consisted of two samples of bucchero (4226-109 and 4226-110) in which no trace of superficial decoration remained. The surface of the loner sample (4032-103) was covered by a thin slip ranging from 7 to 10 µm; the EDS spectrum showed a chemical composition similar to the matrix, but with higher Fe content.

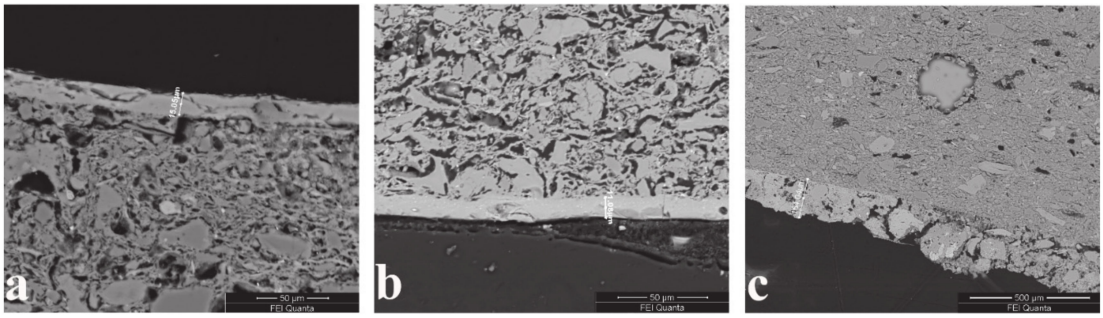

Figure 5. BSE images of slip and ceramic body of representative samples: (**a**) initial vitrification stage of ceramic body and homogeneous and compact slip (sample 4026-102); (**b**) extensive vitrification stage of ceramic body and homogeneous and compact slip (4032-104), (**c**) not vitrified body and porous slip (4226-108).

EMP analysis of the black-gloss ware is reported in Table 4 highlighting the differences among ceramic body and slip. Chemical results showed that the matrix has high amounts of SiO_2 (48.33 wt.%–59.98 wt.%) and Al_2O_3 (16.98 wt.%–20.05 wt.%) and variable CaO (4.74 wt.%–12.98 wt.%).

Table 4. Electron microprobe analysis (EMP) composition of slip and bodies from the different ceramic samples. Concentrations in wt.%.

Sample.	4026-102		4032-158		4226-106		4032-103		4032-104		4032-105		4032-101	
	Slip	Body	Slip	Body	Slip	Body	Slip	Body	Slip	Body	Slip	Body	Slip	Body
SiO_2	48.50	53.50	46.23	55.56	46.56	57.18	46.09	56.47	46.70	59.98	44.97	58.43	47.23	48.33
TiO_2	0.452	0.55	0.54	0.78	0.42	0.68	0.39	0.76	0.67	0.64	0.60	0.32	0.40	0.74
Al_2O_3	28.63	19.72	27.81	20.05	28.32	17.12	30.72	16.98	27.83	18.92	27.57	19.17	27.84	17.58
MgO	2.75	4.21	2.28	2.59	2.17	2.73	1.56	3.58	2.41	1.57	2.02	2.35	2.44	5.75
CaO	0.69	7.79	0.56	7.90	0.83	12.98	1.70	10.22	0.98	5.75	0.97	4.74	0.94	6.53
MnO	0.17	0.04	0.12	0.09	0.09	0.14	0.31	0.31	0.29	0.27	0.99	0.09	0.09	1.48
FeO	13.15	8.55	13.11	3.53	12.32	5.73	12.58	7.44	14.54	5.31	13.87	6.94	11.91	16.48
CuO	0.03	0.10	0	0.02	0.03	0	0.01	0.01	0.01	0.01	0.02	0	0.02	0.03
ZnO	0.06	0.12	0.10	0.07	0.10	0.07	0.04	0.02	0.04	0.11	0.04	0.01	0.12	0.04
Na_2O	0.50	1.45	1.73	0.99	0.86	0.79	0.43	0.66	1.71	2.42	0.80	1.68	0.65	0.18
K_2O	5.07	3.98	7.52	8.42	8.30	2.58	6.17	3.56	4.83	5.05	8.15	5.28	8.37	2.87
Total:	100	100	100	100	100	100	100	100	100	100	100	100	100	100
Al/Si	0.6	0.4	0.6	0.4	0.6	0.3	0.7	0.3	0.6	0.3	0.6	0.3	0.6	0.4

In addition, the body shows a general moderate content of Na_2O (0.66–1.68 wt.%) except for sample 4032-104 with a content of 2.42 wt.% and high concentrations of K_2O (2.58–8.42 wt.%). MgO concentration varies between 1.57 wt.% and 5.75 wt.%, MnO content between 0.04 wt.% and 1.48 wt.%, TiO_2 ranges from 0.32 wt.% to 0.78 wt.%, and ZnO between 0.008 wt.% and 0.121 wt.%.

CaO content indicates that ceramic can be mainly defined as calcareous, except for black-gloss ware from Pompeii (4032–105 and 4032–104), in which the percentage is lower than 6 wt.% [55]. In addition, the amount of fluxes (K_2O, FeO, CaO, MgO, and TiO_2) is greater than 9 wt.%, allowing the clays to be classified as low refractory [55,56].

Black-gloss ware slips showed a decrease in SiO_2 and CaO and an increase in FeO and Al_2O_3 with respect to the body. The other elements did not show considerable variations between body and slip.

SEM images (Figure 5) allowed the evaluation of the vitrification level of both the slip and ceramic body. Black-gloss ware samples showed quite a homogeneous compact slip, whereas bucchero samples showed a thicker superficial layer, neither homogeneous nor compact. Black-gloss ware samples

showed an "initial vitrification" of the ceramic body, as defined by Maniatis and Tite [55], by the appearance of isolated smooth-surfaced areas, more "extensive" [55] in sample 4032-104 in which rare slight buckling and rounding of the edges of the clay plates are observed. On the contrary, in the bucchero samples the body did not show any evidence of the vitrification process.

5. Discussion

5.1. Production Technology

The combined application of OM, XRPD, SEM-EDS, and EMPA gave an exhaustive picture about the general production technology as well as the different technological knowledge related to the superficial decorations.

Concerning fabric A-fine, the abundant presence of very fine inclusions suggests that the vessels were produced starting from a depurated clay. The unimodal grain size distribution excludes an intentional addition of tempers by the ancient potters [29]. Among them, only one bucchero sample showed rare foraminifera probably due to a not accurate depuration of the starting clay or a different supply of the raw materials.

The optical microscopy analysis evidenced that only a few samples show rare calcareous inclusions, however the calcium oxide amount recorded by means of EMPA is from 4.74 to 12.98 wt.%, suggesting the clay raw material used for the studied ceramics were calcareous clays with finely dispersed calcium carbonate. Fabric B-coarse showed similar composition to the other samples, with predominant quartz, K-feldspar, and a unimodal grain size distribution, excluding temper addition. However, the coarser grain size with respect to fabric A-fine suggests a different supply source, as confirmed by the presence of flint fragments. The presence of flint in these samples could be related to sand or sedimentary rocks found along the Sarno river, suggesting a probable provenance related to this area [49].

Finally, the Apulian kylix is distinguished by the diffuse presence of planktonic foraminifera and of some coarser fragments of rocks, the latter strongly confirming the absence of clay purification. A fossiliferous clay can be hypothesized, also supported by the high amount of CaO.

The absence of clay pallets in OM analysis indicates that after material selection, the paste was properly mixed with water for a long time and with a good clay/water ratio [32]. After the mixing, the ceramic was shaped using the potter's wheel, as testified by the regular thickness of vessel walls, the circular traces on the surface and the presence of elongated pores aligned to the margin of the section [45].

Then, a fine suspension of purified clay was applied on the dry surface [18] and finally, the vessels were fired. The levigation process is supported by the decrease of SiO_2 and CaO in the glass, and a consequent increase of illitic components.

All the samples of fabric A-fine showed optical inactivity of the matrix, giving a preliminary information about a firing temperature exceeding 800 °C [45], as suggested by the absence of clay minerals which should be completely degraded in calcareous clay at this temperature [57].

Regarding about black-gloss ware samples, the rare occurrence of calcite and gehlenite suggests a firing temperature close to the upper limit of the decarbonation range, at about 850–900 °C, at which the formation of neo-formed calcium silicates or calcium aluminium silicates [58,59] takes place. At these firing conditions, the ceramic body is made of amorphous material and the formation of gehlenite occurs through reaction of this amorphous material with calcium oxide, originated from decomposition of calcite around. In addition, gehlenite is also formed by the reaction at the edge of relatively very rare coarse calcite inclusions, as observed in sample 4226-106. The "initial vitrification" observed in SEM images strongly supports the hypothesis of a firing temperature in this range for all BGW, close to 900 °C for the Pompeian plate. However, the decarbonation is strongly influenced by different variables connected to the firing procedure (heating rate, steam, oxygen concentration, etc.) and the nature of carbonates (particle size, quantity, crystalline structure, etc.) [60]. Therefore, a firing exposure not long enough to complete the decomposition of calcareous compounds is hypothesized. Furthermore,

the obliteration of the internal structure of microfossils and the occurrence of reactions rims as observed in experimental firings [61–63], strongly support a firing temperature above 850 °C [64], in agreement with literature [8].

On the contrary, the absence of gehlenite in the bucchero samples suggests a lower temperature range, as also confirmed by the absence of "vitrification" of ceramic bodies and the porous slip.

Two different firing atmospheres can be attested: black-gloss ware includes samples showing color matrix ranging from red to brown, with high amounts of nodules of iron oxides, typical of oxidizing conditions, whereas bucchero samples show a dark black matrix due to reducing conditions.

Concerning black-gloss ware, an oxidizing–reducing–oxidizing cycle is proposed. During the first oxidizing phase, the temperature is high enough to induce carbonates and clay minerals decomposition, turning both the body and slip red; when the maximum temperature is reached, a reducing atmosphere is created avoiding the diffusion of oxygen and favouring the formation of the reducing phases. At the same time, aluminosilicates in the slip form an impermeable layer to volatiles. Particle size favours the compactness and smoothness at a lower temperature than that needed for the body [14]. Finally, the third step corresponds to the introduction of oxygen. The oxidizing conditions allow the re-oxidation of the matrix body, which turns to a reddish color, whereas the vitrified layer prevents the re-oxidation of the surface in the third firing step or during the cooling. The shiny surface is connected to the presence of amorphous aluminosilicates in which black phases are embedded [18].

The comparison of chemical data on slip and body do not normally allow us to define if the slip was obtained by depuration of the same clay or by the selection of a different purified clay with specific features. Experiments [12] in simulated slip production proved the difficulty of the levigation process to entirely remove the amount of CaO finely dispersed in the natural clay. However, the higher Al/Si ratio and the enrichment of K in the slip respect to the body in the samples found at Pompeii could be considered a clue to the high amount of illitic components in the clay used for the slip [14].

The high concentration of CaO in the slip of the Apulian kylix could be related to a poor-quality slip probably due to failure in carbonates removal during the refining process [14]. Finally, the absence of Zn in the analyzed samples allowed to exclude the acid treatment of the clay with Pliny's white vitriol (zinc sulfate) observed in Attic samples probably used during the refining process [65].

5.2. Provenance

Some accidental minerals are rather rare, and therefore defined as markers of well-defined geographical areas characterized by specific geological and mineralogical features [8,65]. Therefore, the mineralogical and chemical results of black gloss Pompeian ware are used to verify the archaeological hypothesis about different production areas (Figure 6).

The fine grain size of the ceramic body has made a challenge in which scanning electron microscopy and microanalysis were extremely helpful to identify specific markers.

The sample 4032-101 shows the mineralogical association of Ca-plagioclase, biotite, iron oxides, and zircon, which could agree with the archaeological hypothesis of an Etruscan production, from Pyrgi, a port city on the slopes of the volcanic domain of the Tolfa Mountains [66].

Samples 4026-102 and 4032-158 are hypothesized from central Italy and southern Latium, respectively. SEM-EDS analysis revealed the mineralogical associations of K-feldspar, titanium oxides, clinopyroxene (probably augite), and amphibole as regards the first sample, and of K-feldspar, iron and titanium oxides, clinopyroxene, and zircon as regards the second.

The areas of origin of the three samples just mentioned are linked to the intermediate Apennine unit, characterized by aquifers consisting mainly of Cretaceous clastic deposits and a carbonate platform that affects the Campania-Latium area [49].

Figure 6. Map showing the probable areas of provenance suggested by the results of this work. Sample 4032-101: Pyrgi; samples 4026-102: central Italy; sample 4032-158: southern Latium; sample 4226-106: Cales; sample 4032-103: North-western Apulia; samples 4032-104, 4032-105, 4226-108, 4226-109, 4026-110: Pompeii (blue); sample 4026-107: Salerno area (light blue).

The samples identified as Pompeian production (4032-105, 4032-104, 4020-107, 4226-108, 4226-109, and 4026-110), confirmed the presence of mafic minerals such as clinopyroxene and biotite and of Ca-plagioclase. Quartz and K-feldspar in association with garnet and zircon can be correlated to a high mature sandy sediment enriched in hard and resistant minerals, probably associated with intermediate volcanic products [67]. In addition, the low-Ca paste, typical of the so called Campanian A, further confirms the exclusive production in the Gulf of Naples [8]. Differently, the clay containing foraminifera used for sample 4026-107 was not available close to the site. This is typical of calcareous marine clays in which the occurrence of volcanic inclusions is related to an area affected by the fall of the Vesuvian ashes, i.e., the area of Salerno, not far from Pompeii [68].

One of the BGW plates is supposedly from Cales, close to the now called Calvi Risorta and located 70 Km north-west of Pompeii. EMP analysis on the ceramic body revealed the highest percentage of CaO, possibly correlated to the limestones outcropping in that area.

The presence of abundant planktonic foraminifera fragments within the sample 4032-103 could confirm the Apulian production, as the region stands on a carbonate platform [49]. However, lithic fragments associated with iron and titanium minerals, such as ilmenite, and other minerals typical of igneous rocks have been identified. The mineralogical composition could therefore drive to the hypothesis of a production carried out in local Apulian workshops, close to the Vesuvian volcanic context.

6. Conclusions

The multi-analytical approach including OM, XRPD, SEM-EDS, and EMPA on some black-wares from the temple of Venus Fisica allowed the identification of their production technology and provenance.

Concerning black-gloss ware, the vessels were produced starting from a depurated clay, less accurate for the Apulian kylix; after an appropriate mixing step, the vases were moulded

by the potter's wheel. Then, a fine suspension of purified clay was applied on the dry surface and fired at about 850–900 °C in an oxidizing-reducing-oxidizing cycle.

The bucchero samples were produced with either very refined or less depurated clay (fabric A-fine and fabric B-coarse, respectively), possibly coming from different supply sources. The clay was appropriately mixed and then moulded using the potter's wheel. A suspension of purified clay was applied on the dry surface; however, the suspension was probably less refined respect to the black-gloss ware. The vessels were fired in the range 750–850 °C under reducing conditions avoiding the vitrification of the slip, completely or almost completely.

Despite the fine grain size of the ceramic body, SEM-EDS and EMPA were extremely helpful to define specific mineralogical and chemical markers useful to verify the hypothesized provenances.

The locally produced ceramics, both black-gloss ware and bucchero, have been recognized thanks to the presence of garnet and clinopyroxene, which are typical minerals of the leucitic lavas of the Pompeian area. Those samples that differ in the presence of foraminifera were probably made using limestone clays from the nearby Salerno area.

The Apulian kylix reflects the composition of local carbonate rocks due to the abundance of foraminifera in calcareous clasts. However, the identification of iron and titanium oxides suggests that the clays from Apulian sediments was the closest to the Vesuvian area.

Finally, the mineralogical association in the samples identified as central-Italian production, from the Etruscan city of Pyrgi and from southern Latium, reflects the composition of clastic and carbonate deposits of the Apennine Campanian-Latium unit.

Author Contributions: Conceptualization, L.M.; methodology, C.D.V.; formal analysis, L.M.; investigation, L.M., S.M., and G.D.F.; resources, C.D.V.; data curation, G.D.F., M.B., and C.D.V.; writing—original draft preparation, L.M. and S.M.; writing—review and editing, M.B., F.C., and C.D.V.; funding acquisition, L.M. All authors have read and agreed to the published version of the manuscript.

Funding: This research was funded by Sapienza University of Rome, grant Medeghini 2018.

Acknowledgments: Authors are grateful to the Editor and the anonymous reviewers for their suggestions to improve the manuscript.

Conflicts of Interest: The authors declare no conflict of interest.

References

1. Morel, J.P. La produzione della ceramica campana: Aspetti economici e sociali. In *Società Romana e Produzione Schiavistica, II. Merci, Mercati e Scambi nel Mediterraneo*; Giardina, A., Schiavone, A., Eds.; Laterza: Bari, Italy, 1981; pp. 81–97.
2. Guerrini, C.; Mancini, L. La ceramica di età romana. In *Introduzione Allo Studio Della Ceramica in Archeologia*; Dipartimento di Archeologia e Storia delle Arti, Università di Siena, Centro Editoriale Toscano sas: Firenze, Italy, 2007; pp. 197–234. ISBN 88-86796-47-1.
3. Lollini, D. Bucchero in Encicl. dell'Arte Antica Ebook. In *Treccani*; Treccani: Rome, Italy, 1959.
4. Rotroff, S.I. *The Athenian Agora: Results of Excavations Conducted by the American School of Classical Studies at Athens. Volume XXXIII. Hellenistic Pottery: The Plain Wares*; The American School of Classical Studies at Athens: Princeton, NJ, USA, 2006.
5. Gliozzo, E.; Kirkman, I.W.; Pantos, E.; Turbanti, I.M. Black gloss pottery: Production sites and technology in northern Etruria, part II: Gloss technology. *Archaeometry* **2004**, *46*, 227–246. [CrossRef]
6. Morsiani, S. Ceramica a vernice nera. In *Pompei. Insula IX 8. Vecchi e Nuovi Scavi (1879-)*; Coralini, A., Ed.; Ante Quem: Bologna, Italy, 2017; pp. 569–586. ISBN 9788878491151.
7. Lamboglia, N. *Per una classificazione preliminare della Ceramica Campana*; Istituto Internazionale di Studi Liguri: Bordighera, Imperia, Italy, 1952; pp. 1–68.
8. Montana, G.; Tsantini, E.; Randazzo, L.; Burgio, A. SEM-EDS analysis as a rapid tool for distinguishing Campanian A ware and sicilian imitations. *Archaeometry* **2013**, *55*, 591–608. [CrossRef]
9. Morel, J.P.M. *Céramique Campanienne: Les Formes*; École Française de Rome: Rome, Italy, 1981.

10. Brecciaroli Taborelli, L. Ceramiche a Vernice Nera. In *La ceramica e i Materiali di Età Romana. Classi, Produzioni, Commerci e Consumi*; Gandolfi, D., Ed.; Ist. Studi Liguri: Bordighera, Imperia, Italy, 2005; pp. 59–75. ISBN 978-8886796477.
11. Maggetti, M.; Galetti, G.; Schwander, H.; Picon, M.; Wessicken, R. Campanian pottery: The nature of the black coating. *Archaeometry* **1981**, *23*, 199–207. [CrossRef]
12. Maniatis, Y.; Aloupi, E.; Stalios, A.D. New evidence for the nature of the Attic Black Gloss. *Archaeometry* **1993**, *35*, 23–34. [CrossRef]
13. Vendrell-Saz, M.; Pradell, T.; Molera, J.; Aliaga, S. Proto-Campanian and A-Campanian ceramics: Characterization of the differences between the black coatings. *Archaeometry* **1991**, *33*, 109–117. [CrossRef]
14. Mirti, P.; Casoli, A.; Calzetti, L. Technology of production of fine pottery excavated on a western Greek site investigated by scanning electron microscopy coupled with energy-dispersive X-ray detection. *X-Ray Spectrom.* **1996**, *25*, 103–109. [CrossRef]
15. Mirti, P.; Casoli, A.; Barra Bagnasco, M.; Preacco Ancona, M.C. Fine ware from Locri Epizephiri: A provenance study by Inductively Coupled Plasma Emission Spectroscopy. *Archaeometry* **1995**, *37*, 41–51. [CrossRef]
16. Prag, A.J.N.W.; Schweizer, F.; Williams, J.L.W.; Schubiger, P.A. Hellenistic glazed wares from Athens and southern Italy: Analytical techniques and implications. *Archaeometry* **1974**, *16*, 153–187. [CrossRef]
17. Mirti, P.; Davit, P. Technological characterization of Campanian pottery of type A, B and C and of regional products from ancient Calabria (Southern Italy). *Archaeometry* **2001**, *43*, 19–33. [CrossRef]
18. Tang, C.C.; MacLean, E.J.; Roberts, M.A.; Clarke, D.T.; Pantos, E.; Prag, A.J.N.W. The study of Attic black gloss sherds using synchrotron x-ray diffraction. *J. Archaeol. Sci.* **2001**, *28*, 1015–1024. [CrossRef]
19. Rasmussen, T.B. *Bucchero Pottery from Southern Etruria*; Cambridge University Press: Cambridge, UK, 1979; ISBN 9781107297944.
20. Maiuri, A. Saggi nell'area del tempio di Apollo. *Mem. dei Lincei* **1943**, *IV*, 123–149.
21. Stefano, D.C. *Saggi nell'area del Tempio di Apollo a Pompei Scavi Stratigrafici di A. Maiuri 1931-32, 1942–43*; Istituto Universitario Orientale, Dipartimento Di Studi Del Mondo Classico E Del: Napoli, Italy, 1986.
22. Francaviglia, V.; Minardi, M.E.; Palmieri, A. Comparative study of various samples of Etruscan Bucchero by X-ray Diffraction, X-ray Spectrometry and Thermoanalysis. *Archaeometry* **1975**, *2*, 223–231. [CrossRef]
23. Tite, M.S. Pottery production, distribution, and consumption—The contribution of the physical sciences. *J. Archaeol. Method Theory* **1999**, *6*, 181–233. [CrossRef]
24. Turbanti Memmi, I. Pottery production and distribution: The contribution of mineralogical and petrographical methodologies in Italy. State of the art and future developments. *Period. Mineral.* **2004**, *73*, 239–257.
25. Patrick, S.Q. *Ceramic Petrography: The Interpretation of Archaeological Pottery and Related Artefacts in Thin Section*; Archaeopress Archaeology: Oxford, UK, 2013; ISBN 978-1905739592.
26. Velde, B.; Druc, I.C. *Archaeological Ceramic Materials: Origin and Utilization*; Springer Science & Business Media: Berlin/Heidelberg, Germany, 2012.
27. Santacreu, D.A.; Vicens, G.M. Raw Materials and Pottery Production at the Late Bronze and Iron Age Site of Puig de Sa Morisca, M allorca, S pain. *Geoarchaeology* **2012**, *27*, 285–299. [CrossRef]
28. Hunt, A.M. *The Oxford Handbook of Archaeological Ceramic Analysis*; Oxford University Press: Oxford, UK, 2017.
29. De Vito, C.; Medeghini, L.; Mignardi, S.; Ballirano, P.; Peyronel, L. Technological fingerprints of the Early Bronze Age clay figurines from Tell Mardikh-Ebla (Syria). *J. Eur. Ceram. Soc.* **2015**, *35*, 3743–3754. [CrossRef]
30. Ion, R.M.; Dumitriu, I.; Fierascu, R.C.; Ion, M.; Pop, S.F.; Radovici, C.; Bunghez, R.I.; Niculescu, V.I.R. Thermal and mineralogical investigations of historical ceramic: A case study. *J. Therm. Anal. Calorim.* **2011**, *104*, 487–493. [CrossRef]
31. De Benedetto, G.E.; Laviano, R.; Sabbatini, L.; Zambonin, P.G. Infrared spectroscopy in the mineralogical characterization of ancient pottery. *J. Cult. Herit.* **2002**. [CrossRef]
32. Forte, V.; Medeghini, L. A preliminary study of ceramic pastes in the copper age pottery production of the Rome area. *Archaeol. Anthropol. Sci.* **2017**, *9*, 209–222. [CrossRef]
33. Quinn, P.; Day, P.; Kilikoglou, V.; Faber, E.; Katsarou-Tzeveleki, S.; Sampson, A. Keeping an eye on your pots: The provenance of Neolithic ceramics from the Cave of the Cyclops, Youra, Greece. *J. Archaeol. Sci.* **2010**, *37*, 1042–1052. [CrossRef]
34. Quinn, P.S.; Burton, M.M. Ceramic distribution, migration and cultural interaction among late prehistoric (ca. 1300–200 B.P.) hunter-gatherers in the San Diego region, Southern California. *J. Archaeol. Sci. Reports* **2016**, *5*, 285–295. [CrossRef]

35. Tite, M.S.; Maniatis, Y. Examination of ancient pottery using the scanning electron microscope. *Nat. Publ. Gr.* **1975**, *257*, 122–123. [CrossRef]
36. Enea-Giurgiu, A.; Ionescu, C.; Hoeck, V.; Tudor, T.; Roman, C. An archaeometric study of early Copper Age pottery from a cave in Romania. *Clays Clay Miner.* **2019**, *54*, 255–268. [CrossRef]
37. Ferreira, L.F.V.; Gonzalez, A.; Pereira, M.F.C.; Santos, L.F.; Casimiro, T.M.; Ferreira, D.P. Spectroscopy of 16th century Portuguese tin-glazed earthenware produced in the region of Lisbon. *Ceram. Int.* **2015**, *41*, 13433–13446. [CrossRef]
38. Barilaro, D.; Barone, G.; Crupi, V.; Donato, M.G.; Majolino, D.; Messina, G.; Ponterio, R. Spectroscopic techniques applied to the characterization of decorated potteries from Caltagirone (Sicily, Italy). *J. Mol. Struct.* **2005**, *744*, 827–831. [CrossRef]
39. Medeghini, L.; Fayek, M.; Mignardi, S.; Coletti, F.; Contino, A.; De Vito, C. A provenance study of Roman lead-glazed ceramics using lead isotopes and secondary ion mass spectrometry (SIMS). *Microchem. J.* **2020**, *154*, 104519. [CrossRef]
40. Dorais, M.J.; Lindblom, M.; Shriner, M. Evidence for a single clay/temper source for the manufacture of Middle and Late Helladic Aeginetan pottery from Asine, Greece. *Geoarchaeology* **2004**, *19*, 657–684. [CrossRef]
41. Barone, G.; Belfiore, C.M.; Mazzoleni, P.; Pezzino, A.; Viccaro, M. A volcanic inclusions based approach for provenance studies of archaeological ceramics: Application to pottery from southern Italy. *J. Archaeol. Sci.* **2010**, *37*, 713–726. [CrossRef]
42. Belfiore, C.M.; La Russa, M.F.; Barca, D.; Galli, G.; Pezzino, A.; Ruffolo, S.A.; Viccaro, M.; Fichera, G. V A trace element study for the provenance attribution of ceramic artefacts: The case of Dressel 1 amphorae from a late-Republican ship. *J. Archaeol. Sci.* **2014**, *43*, 91–104. [CrossRef]
43. Fabrizi, L.; Nigro, L.; Ballirano, P.; Guirguis, M.; Spagnoli, F.; Medeghini, L.; De Vito, C. The Phoenician Red Slip Ware from Sulky (Sardinia-Italy): Microstructure and quantitative phase analysis. *Appl. Clay Sci.* **2020**, *197*, 105795. [CrossRef]
44. De Vito, C.; Medeghini, L.; Mignardi, S.; Coletti, F.; Contino, A. Roman glazed inkwells from the "Nuovo Mercato di Testaccio" (Rome, Italy): Production technology. *J. Eur. Ceram. Soc.* **2017**, *37*, 1779–1788. [CrossRef]
45. De Vito, C.; Medeghini, L.; Garruto, S.; Coletti, F.; De Luca, I.; Mignardi, S. Medieval glazed ceramic from Caesar's Forum (Rome, Italy): Production technology. *Ceram. Int.* **2018**, *44*, 5055–5062. [CrossRef]
46. Curti, E. Le aree portuali di Pompei: Ipotesi di lavoro. In *Suburbio 'portuale' di Pompei*; Scarano Ussani, V., Ed.; Loffredo Editore: Napoli, Italy, 2005; pp. 51–76. ISBN 8875641048.
47. Curti, E. Il tempio di Venere Fisica e il Porto di Pompei. In Proceedings of the Atti del Convegno Internazionale "Nuove ricerche archeologiche nell'area vesuviana (scavi 2003–2006)", Roma, Italy, 11–3 February 2007; Guzzo, P.G., Guidobaldi, M.P., Eds.; "L'Erma" di Bretschneider: Rome, Italy, 2008; pp. 47–59.
48. Seiler, F.; Märker, M.; Kastenmeier, P.; Vogel, S.; Esposito, D.; Heussner, U.; Boni, M.; Balassone, G.; Maio, G.D.; Joachimski, M. Interdisciplinary approach on the reconstruction of the ancient cultural landscape of the Sarno River Plain before the eruption of Somma-Vesuvius A.D. 79. *Tag Landesmus Vor. Halle* **2011**, *6*, 1–10.
49. ISPRA. Carta Geologica d'Italia. Dai Rilevamenti Geologici 1:10000. Available online: https://www.isprambiente.gov.it/Media/carg/466_485_SORRENTO_TERMINI/Foglio.html (accessed on 20 September 2020).
50. Coletti, F.; Sterpa, G. Resti pavimentali in cementizio, mosaico e sectile dall'area del tempio di Venere a Pompei: Dati di scavo. In Proceedings of the Atti del XIII Colloquio Internazionale dell'AISCOM, Canosa di Puglia, Italy, 21–24 February 2007; Angelelli, C., Massara, D., Sposito, F., Eds.; Scripta Manent: Rome, Italy, 2008; pp. 129–136.
51. Coletti, F.; Prascina, C.; Sterpa, G.; Witte, N. Venus Pompeiana. Scelte progettuali e procedimenti tecnici per la realizzazione di un grande edificio sacro tra tarda Repubblica e primo Impero. In Proceedings of the Atti del workshop "Arqueología del la Costrucciòn, II. Los procesos constructivos en el mundo romano: Italia y Provincias Orientales", Certosa di Pontignano-Siena, Italy, 13–15 November 2008; Camporeale, S., Dessales, H., Pizzo, A., Eds.; Consejo Superior de Investigaciones: Taravilla, Madrid, Spain, 2010; pp. 189–211.
52. Coletti, F. Ceramica a vernice nera a Pompei. Il caso dei depositi votivi del santuario di Venere Fisica: Produzione, circolazione, mercati. Un primo bilancio. In *Fecisti Cretaria: Dal Frammento al Contesto Studi Sul Vasellame Ceramico del Territorio Vesuviano*; Osanna, M., Toniolo, L., Eds.; "L'Erma" di Bretschneider: Rome, Italy, 2020; pp. 77–95.

53. Whitbread, I.K. *Greek Transport Amphorae: A Petrological and Archaeological Study*; British School at Athens: Athina, Greece, 1995; ISBN 0904887138.
54. Pouchou, J.L.; Pichoir, F. "PAP" procedure for improved quantitative microanalysis. In *Microbeam Analysis*; Armstrong, J.T., Ed.; San Francisco Press: San Francisco, CA, USA, 1985; pp. 104–106.
55. Maniatis, Y.; Tite, M. Technological studies of Neolithic-Bronze Age Pottery from Central and Southeast Europe and from the Near East. *J. Archaeol. Sci.* **1981**, *8*, 59–76. [CrossRef]
56. Musthafa, A.M.; Janaki, K.; Velraj, G. Microscopy, porosimetry and chemical analysis to estimate the fi ring temperature of some archaeological pottery shreds from India. *Microchem. J.* **2010**, *95*, 311–314. [CrossRef]
57. Aras, A. The change of phase composition in kaolinite- and illite-rich clay-based ceramic bodies. *Appl. Clay Sci.* **2004**, *24*, 257–269. [CrossRef]
58. Rathossi, C.; Pontikes, Y. Effect of firing temperature and atmosphere on ceramics made of NW Peloponnese clay sediments. Part I: Reaction paths, crystalline phases, microstructure and colour. *J. Eur. Ceram. Soc.* **2010**, *30*, 1853–1866. [CrossRef]
59. Medeghini, L.; Mignardi, S.; De Vito, C.; Macro, N.; D'Andrea, M.; Richard, S. New insights on Early Bronze Age IV pottery production and consumption in the southern Levant: The case of Khirbat Iskandar, Jordan. *Ceram. Int.* **2016**, *42*, 18991–19005. [CrossRef]
60. Karunadasa, K.S.P.; Manoratne, C.H.; Pitawala, H.M.T.G.A.; Rajapakse, R.M.G. Thermal decomposition of calcium carbonate (calcite polymorph) as examined by in-situ high-temperature X-ray powder diffraction. *J. Phys. Chem. Solids* **2019**, *134*, 21–28. [CrossRef]
61. Privitera, A.; Guido, A.; Mastandrea, A.; Rao, A.; Russo, F. Morphological and mineralogical evolution of microfossils during the heating process: A contribution to the archaeometric study of ceramics. *Rend. Fis. Acc. Lincei* **2015**, *26*, 499–512. [CrossRef]
62. Tenconi, M.; Maritan, L.; Donadel, V.; Angelini, A.; Leonardi, G.; Mazzoli, C. Evolution of the ceramic production at the Alpine site of Castel de Pedena: Technology and innovation between the Recent Bronze Age and the early Iron Age. *Archaeol. Anthropol. Sci.* **2017**, *9*, 965–984. [CrossRef]
63. Maritan, L.; Mazzoli, C.; Freestone, I. Modelling changes in mollusc shell internal microstructure during firing: Implications for temperature estimation in shell-bearing pottery. *Archaeometry* **2007**, *49*, 529–541. [CrossRef]
64. Maritan, L.; Zamparo, L.; Mazzoli, C.; Bonetto, J. Punic black-gloss ware in Nora (south-western Sardinia, Italy): Production and provenance. *J. Archaeol. Sci. Reports* **2019**, *23*, 1–11. [CrossRef]
65. Gianoncelli, A.; Raneri, S.; Schoeder, S.; Okbinoglu, T.; Barone, G.; Santostefano, A.; Mazzoleni, P. Synchrotron μ-XRF imaging and μ-XANES of black-glazed wares at the PUMA beamline: Insights on technological markers for colonial productions. *Microchem. J.* **2020**, *154*, 104629. [CrossRef]
66. Laurora, A.; Brigatti, M.F.; Mottana, A.; Malferrari, D.; Caprilli, E. Crystal chemistry of trioctahedral micas in alkaline and subalkaline volcanic rocks: A case study from Mt. *Sassetto (Tolfa district, Latium, central Italy).* **2020**, *92*, 468–480. [CrossRef]
67. Kastenmeier, P.; Di Maio, G.; Balassone, G.; Boni, M.; Joachimski, M.; Mondillo, N. The source of stone building materials from the Pompeii archaeological area and its surroundings. *Period. Mineral.* **2010**, *79*, 39–58. [CrossRef]
68. Schneider, G.; Daszkiewicz, M.; Cottica, D. Pompeii as a pottery production centre. An archaeometric approach. *Rei Cretariae Rom. Fautorum Acta* **2010**, *41*, 313–318.